Kinetic Study on the Poly(methyl methacrylate) Seeded Soapless Emulsion Polymerization of Styrene. III. Seeds with Crosslinking

CHIA-FEN LEE, WEN-YEN CHIU

Department of Chemical Engineering, National Taiwan University, Taipei, Taiwan, Republic of China

Received 27 July 1995; accepted 6 December 1996

ABSTRACT: In this work, a seeded soapless emulsion polymerization was carried out with crosslinking (XL) poly(methyl methacrylate) (PMMA) as seeds, styrene as monomer, and potassium persulfate ($K_2S_2O_8$) as initiator to synthesize the PMMA XL–PS composite latex, which we knew as the latex interpenetrating polymer network (IPN). The morphology of the latex IPN was observed by transmission electron microscopy (TEM). It showed a core–shell structure. The kinetic data from the early stages of the reaction of seeded soapless emulsion polymerization showed that the square root of polymer yield $(W_p)^{1/2}$ was proportional to the reaction time. The reaction rate decreased with the increase of crosslinking density of PMMA seeds. The core–shell model proposed in our previous work[1–2] was modified to predict the conversion of polymerization over the entire course of the synthesis of PMMA(XL)–PS composite latex. Our modified core–shell kinetic model fitted well with the experimental data. © 1997 John Wiley & Sons, Inc. J Appl Polym Sci **65:** 425–438, 1997

INTRODUCTION

In recent years, the interpenetrating polymer networks (IPNs) have been extensively investigated to improve the degree of mixing of the multiphase polymer materials. The IPNs have a very limited processability and thus can only be used as made.[1] In recent years, much attention has been focused on the synthesis of latex IPNs. The latex IPNs were processable by the particle–slippage flow mechanism.

The latex IPNs were synthesized by the method of seeded emulsion polymerization, where the first monomer was emulsion-polymerized and crosslinked to form a seed latex. A second monomer was added to the seed latex and then polymerized without forming new particles.[2–4] There were many factors to control the morphology of latex IPNs, such as the method of monomer added in system,[5] the sequence of monomers fed in system, the monomer ratio in two stages, the hydrophilicity of monomers, the surface tension, the molecular weight of polymers,[5–7] the compatibility of polymers,[8] and properties of initiators.[9] H. R. Shen et al.[18] investigated the synthesis of polystyrene–polystyrene latex IPNs. They pointed out that the appearance morphology of latex was uneven because phase separation occurred between polymer I and polymer II during polymerization. From 1968 to 1973,[10–12] many researchers investigated the synthesis of ABS (styrene-co-acylonitrile) semi-IPN latex by the method of seeded emulsion polymerization. They used crosslinked polybutadiene (PB) as seeds and used styrene and acrylonitrile as monomer II. They found that in the ABS latex, the SAN (acylonitrile-butadiene-styrene) microdomain distributed in the PB matrix.

Flory and Stockmayer[13] pointed out the kinetic model for the free radical crosslinking polymeriza-

Correspondence to: Wen-Yen Chiu

 CCC 0021-8995/97/030425-14

Table I Ingredients and Conditions for the Synthesis of Seed Latex (First Stage)

Ingredients	Conditions
Methyl methacrylate (g)	120
Initiator ($K_2S_2O_8$)	0.866
Crosslinking agent (EGDMA) (g)	7.929–2.798
Deionized water (g)	1100
Temperature (°C)	70
Stirring rate (rpm)	300
Reaction method	Batch

tion. In 1990, H. Tobita and A. E. Hamielec[14] investigated the crosslinking kinetic model for bulk polymerization and emulsion polymerization. They pointed out that the difference between bulk and emulsion polymerization was that the reaction rate of the former was slower than the latter because at high conversion, the viscosity of the bulk polymerization was high and the efficiency of initiator was low. D. Zou et al., in 1990–1992,[15–17] investigated the synthesis of crosslinking latex. They found that different monomers possessed different kinetic models, but the same was that the reaction rate increased with the increase of crosslinking density.

In this work, the core–shell latex IPNs were synthesized with crosslinking cores and linear shells. The core–shell model proposed in our previous work[2–3] was modified to predict the rate of polymerization over the entire course of the synthesis of latex IPNs.

EXPERIMENTAL

Material

Methyl methacrylate and styrene were distilled under nitrogen atmosphere and reduced pressure prior to polymerization. The crosslinking agent used in this work was ethyleneglycol dimethacrylate (EGDMA). Water was redistilled and deionized. Other chemicals were of analytical grade and used without further purification.

Ingredients and conditions for the synthesis of seed latex (first stage) is listed in Table I. Table II lists the ingredients and conditions for the synthesis of composite latex in seeded polymerization (second stage).

Polymerization

Two-stage polymerization reactions were carried out with the detailed procedures mentioned in our previous work.[2–3] The first stage was to synthesize the crosslinking PMMA seed latex; the ingredients and conditions for polymerization are shown in Table I. After the reaction of first stage was complete, then the seed latex was quenched to room temperature. In the second stage of reaction, as seen in Table II, quantitative styrene was added into the seed latex, and the seeds were swollen for 24 hours at room temperature. Then the reaction system was heated in a water batch at the temperature of reaction. The aqueous solution of $K_2S_2O_8$ was added into the reaction after the temperature of the system reached the temperature of reaction, and the reaction of second stage began.

Conversion

At a certain time during the second stage of polymerization, a sample of the emulsion latex was taken out of the reactor and poured into methanol with hydroquinone to stop the reaction. The precipitated polymers were washed with methanol and water several times, then dried in a vaccum oven.

The conversion of the seeded polymerization was calculated as follows:

$$\text{conversion } (x) = \frac{W_2 - W_1 \times B\%}{W_1 \times M_o(\text{ST})\%}$$

where W_1 is the weight of sample taken from the vessel; W_2, the weight of dry polymers obtained from the taken sample; $M_o(\text{ST})\%$, the weight percentage of the styrene monomer fed into the reaction mixture; and $B\%$, the weight percentage of PMMA in the reaction mixture.

Table II Ingredients and Conditions for the Synthesis of Composite Latex in Seeded Polymerization (Second Stage)

Ingredients	Conditions
Seed latex (g)	500
Styrene (g)	73.77
Initiator ($K_2S_2O_8$)	0.5
Deionized water (g)	310
Temperature (°C)	70
Stirring rate (rpm)	300
Reaction method	Batch

Particle Size and Size Distribution

The samples taken from the reactor over the course of seeded polymerization of styrene would contain polymer particles and monomer droplets. The styrene monomer droplets could be removed away by centrifugation. The remaining samples then reacted at 90°C for 36 hours with further addition of initiator. The reaction was complete, and the size and size distribution of polymer particles were determined by transmission electron microscopy (TEM).

Observation of Particle Morphology

The latex particles from the seeded polymerization were ultramicrotomed to from sections about 900 Å thick and stained with RuO_4. The stained sections of the latex particles were observed under the TEM. In the TEM photograph, the PMMA phase was light, and the PS phase was dark; this was because the RuO_4 would react with PS but not with PMMA.

Concentration of Monomer in Polymer Particles

A quantitative sample was taken out from the second stage of reaction system, and the aqueous solution of hydroquinone was added into the sample to stop the reaction. The monomer droplets were removed away from the sample by the method of centrifugation. Then, the remaining sample was divided into two equal weight parts.

Quantitative hydroquinone and methanol were added into one part, filtered, and dried in oven at 80°C; the dry sample weight was designated as P. Quantitative $K_2S_2O_8$ was added into another part of sample and reacted in a closed system at 90°C for 36 hours. After the reaction, dried in oven at 80°C, the dry sample weight was designated as Q.

Assuming the volumes of polymer and monomer in polymer particles were additive, then the monomer concentration in polymer particles was calculated as

$$[M]_P = \frac{(Q - P)}{\dfrac{P}{\bar{\rho}_p} + \dfrac{(Q - P)}{\rho_M}} \times \frac{1}{104}$$

where $\bar{\rho}_p$ is the average density of PMMA and polystyrene (PS) (1120.5 g L^{-1}), ρ_M is the density of styrene (905 g L^{-1}),[11] 104 is the molecular weight of styrene, and $[M]_p$ is the monomer concentration in polymer particles.

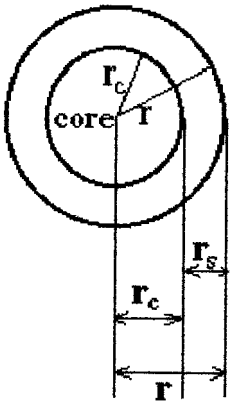

Figure 1 A polymer particle with core–shell regions.

THEORETICAL CONSIDERATION

Core–Shell Model

In our soapless seeded emulsion polymerization system, such as the polymerization of styrene with crosslinking (XL) PMMA latex particles as seeds and $K_2S_2O_8$ as the initiator, the PS polymer chains were initiated by $K_2S_2O_8$; and the functional group (SO_4^-) at the end of polymer chains was hydrophilic, but the polymer chains were hydrophobic. So the hydrophilic group SO_4^- would anchor on the surface of polymer particles, and the reaction loci were on the surface layer.

The morphology of the PMMA (XL)–PS composite latex particles was with the core–shell structure, as seen in Figure 1. We considered the mechanism of the synthesis of the PMMA (XL)–PS composite latex particles being the same as that of linear PMMA–PS composite latex particles. Therefore, the core–shell kinetic model that was proposed in our previous work[2–3] could be used to describe the mechanism and kinetics of the synthesis of core (XL)–shell latex particles in this work.

Assuming that the monomer distributed in the polymer particles uniformly,[2–3] the reaction loci were on the surface layer. When the system still had monomer droplets, the concentration of monomer in polymer particles was retained at saturated concentration. That is because monomers would diffuse quickly from droplets to polymer particles for the reaction of polymerization. But when the monomer droplets disappeared, the

monomer inside the polymer particles had to diffuse outward to the surface layer for the reaction of polymerization. The mechanism described above resulted in the core–shell morphology of polymer particles.

The following diagram showed the core and the shell regions in one polymer particle. The core region was crosslinked PMMA seed swollen with styrene. The shell region was the reaction zone, containing styrene and linear PS formed from the reaction of polymerization where r_c is the radius of core (PMMA + styrene), r is the radius of latex particle, and r_s is the thickness of shell (S + styrene).

During polymerization, the thickness of reaction zone (r_s) or the volume of reaction zone increased with increasing the conversion. The styrene monomer was assumed to be uniformly distributed in either the core or shell region of polymer particles.

From the mass balance of the styrene monomer, we obtained

$$\tfrac{4}{3}\pi r_c^3[M]_c + [M]_s[\tfrac{4}{3}\pi(r^3 - r_c^3)] = \tfrac{4}{3}\pi r^3[M]_p \quad (1)$$

where $[M]_c$ is monomer concentration in core (mol l^{-1}), $[M]_s$ is the monomer concentration in shell (mol l^{-1}), and $[M]_p$ is the average monomer concentration in the polymer particle (mol l^{-1}).

Rate of Polymerization

In our soapless seeded emulsion polymerization, the system contained a fixed number of polymer particles. The core–shell kinetics model that was proposed in our previous work[2-3] described that the shell was the reaction zone; that is, the polymerization reaction took place only on the shell.

Then the rate of polymerization could be expressed as

$$R_p = k_p[M]_s[R\bullet]V_rN \quad (2)$$

where R_p is the rate of polymerization, k_p is the propagation rate constant, $[M]_s$ is the monomer concentration in shell, $[R\bullet]$ is the concentration of radicals in one polymer particle, V_r is the volume of reaction zone in one polymer particle, and N is the number of polymer particles per unit volume of water.

Assuming steady state for all radicals,

$$\rho_i = R_t = k_t[R\bullet]^2V_rN \quad (3)$$

where ρ_i is the generation rate of radicals, R_t is the termination rate of radicals, and k_t is the termination rate constant.

Then

$$[R\bullet] = \left(\frac{\rho_i}{k_tV_rN}\right)^{1/2} \quad (4)$$

and the rate of polymerization R_p is expressed as follows:

$$R_p = k_p[M]_s\left(\frac{\rho_i}{k_tV_rN}\right)^{1/2}V_rN$$

$$= \mathrm{k}_p[M]_s\left(\frac{\rho_iN}{k_t}\right)^{1/2}V_r^{1/2} \quad (5)$$

The total volume of monomer and polymer in the reaction zone is calculated simply by the additivity rule, as follows:

$$V_r = \frac{W_p}{\rho_pN} + \frac{[M]_sV_r\cdot 104}{\rho_M} \Rightarrow$$

$$V_r = \frac{W_p}{\rho_p\left(1 - \dfrac{[M]_s\cdot 104}{\rho_M}\right)N} \quad (6)$$

where W_p is the polymer (PS) yield (grams per liter of water) in seeded polymerization, ρ_p is the density of polymer (PS), ρ_M is the density of styrene monomer, and 104 is the molecular weight of the styrene monomer. Substituting V_r into R_p, we obtained

$$R_p = k_p[M]_s\left(\frac{\rho_i}{k_t}\right)^{1/2}\frac{W_p^{1/2}}{\rho_p^{1/2}\left(1 - \dfrac{[M]_s\cdot 104}{\rho_M}\right)^{1/2}} \quad (7)$$

Three regions were considered over the entire course of polymerization.

Region I ($0 \le x < x_c$)

Assuming that before the monomer droplets disappeared, the styrene monomer concentration distributed in either core or shell region in the polymer particle was saturated. That is, both $[M]_c$ and $[M]_s$ are constants (e.g., $[M]_c^o$ and $[M]_s^o$).

The half-life of $K_2S_2O_8$ was very long, so the

concentration of initiator was assumed to be constant over the polymerization; that is,

$$\rho_i = 2k_d f[I] = \text{constant} \quad (8)$$

where k_d is the constant for the initiator decomposition, f is the initiator efficiency, and $[I]$ is the initiator concentration.

Equation (7) could be rewritten as follows[2–3]:

$$\frac{dx}{dt} = k_{po}[M]_s^o\left(\frac{\rho_i}{k_{to}}\right)^{1/2} \times \frac{x \cdot 104}{[M]_o\rho_p\left(1 - \dfrac{[M]_s^o \cdot 104}{\rho_M}\right)}^{1/2} \quad (9)$$

or

$$\frac{W_p^{1/2} - W_{po}^{1/2}}{t - t_o} = k_{po}[M]_s^o\left(\frac{\rho_i}{k_{to}\rho_p}\right)^{1/2} \times \frac{52}{\left(1 - \dfrac{[M]_s^o \cdot 104}{\rho_M}\right)^{1/2}} \quad (10)$$

where $[M]_o$ is the initial concentration of monomer in the system; $[M]_s^o$ is the monomer concentration in the shell region before the monomer droplets disappeared; W_{po} was the PS yield initially ($t = t_o = 0$) in seeded polymerization; and $k_t = k_{to}$, $k_p = k_{po}$, and $[M]_s$ = constants, respectively, before the gel effect took place.

The $[M]_s$ value would be obtained from the slope of $W_p^{1/2}$ versus t plot. The value of $k_{po}\left(\dfrac{\rho_i}{k_{to}}\right)^{1/2}$ was $7.01 \times 10^{-3}\ \dfrac{1}{\text{min}}\left(\dfrac{l}{l - \text{H}_2\text{O}}\right)^{1/2}$, which was obtained from our previous work.[2]

Region II ($x_c \le x \le x_g$)

Once the monomer droplets disappeared, the $[M]_p$ was no longer constant, and the $[M]_p$ dropped linearly with the conversion. Because the reaction loci were on the surface layer, the monomer inside the polymer particles had to diffuse outward to the surface layer for the reaction of polymerization. But the core region of the polymer particle now was with a crosslinking structure, so the diffusion of monomer concentration in the core region ($[M]_c$) was actually not equal to that in the shell region ($[M]_s$); that is, $[M]_c < [M]_s$.

An empirical equation for $M_s(x)$ describing the relation between the monomer concentration in the shell region and the conversion could be obtained from curve fitting of eq. (7) together with the experimental data, conversion versus time, as follows:

$$[M]_s = M_s(x) \quad (11)$$

$$M_s(x) = [M]_s^o[(1 - x)/(1 - x_c)]^{0.8} \times [\log(1 - x_c)/\log(1 - x)]^{0.4} \quad (12)$$

where x_c is the conversion when the monomer droplets disappeared.

On the other hand, once the monomer droplets disappeared, $[M]_p$ was no longer constant. $[M]_s$ would decrease significantly with increasing the conversion. The viscosity in reaction zone turned higher and higher with increasing the conversion, and the termination must be modified by the empirical equation[1–2]

$$k_t = k_{to}T(x) \quad (13)$$

$$T(x) = \left(\frac{1 - x}{1 - x_c}\right)^2 \exp(-2.7((x - x_c) + (x - x_c)^2)) \quad (\text{at } 70^\circ\text{C}) \quad (14)$$

Substituting eqs. (11)–(14) into eq. (7), we obtained

$$\frac{dx}{dt} = k_{po}M_s(x)\left(\frac{\rho_i}{k_{to}T(x)}\right)^{1/2} \times \left(\frac{x \cdot 104}{[M]_o\rho_p\left(1 - \dfrac{M_s(x) \cdot 104}{\rho_M}\right)}\right)^{1/2} \quad (15)$$

Region III ($x_g \le x < 1.0$)

In the latter period of reaction, the viscosity of the reaction mixture became very high. Even the propagation of monomer was seriously hindered, and the glassy effect was obvious. So the rate constant of propagation (k_p) must be modified empirically as[1–2]

$$k_p = k_{po}P(x) \quad (16)$$

$$P(x) = \exp(-4.3x) \quad (\text{at } 70^\circ\text{C}) \quad (17)$$

Substituting eqs. (11)–(14) and (16)–(17) into eq. (7), we obtained

$$\frac{dx}{dt} = k_{po}P(x)M_s(x)\left(\frac{\rho_i}{k_{to}T(x)}\right)^{1/2} \times \left(\frac{x \cdot 104}{[M]_o\rho_p\left(1 - \frac{M_s(x)\cdot 104}{\rho_M}\right)}\right)^{1/2} \quad (18)$$

Monomer Concentration in the Polymer Particle

In the beginning of polymerization, the system still had lots of monomer droplets, and the concentration of monomer in either core region or shell region in polymer particles was retained at the saturated concentration. That meant that the monomer could diffuse quickly from the monomer droplets to the polymer particles during polymerization.

Once the monomer droplets disappeared, the monomer concentration in the polymer particle would decrease with increasing the conversion. Because the reaction loci were on the shell region of polymer particle, the monomer should diffuse from the core region to the shell region for the reaction of polymerization. And the diffusion of the monomer would be hindered by the crosslinking structure of core; therefore, the monomer concentration in the core region would be larger than that in the shell region; that is, $[M]_c < [M]_s$.

In region II of the polymerization, empirical eqs. (13)–(14) were used to describe the monomer concentration in the shell region. On the other hand, the monomer concentration in the polymer particle could be measured experimentally, which decreased linearly with increasing the conversion, as shown in Figure 7 and eq. (19)

$$[M]_p = [M]_{sa}\frac{1 - x}{1 - x_c} \quad (19)$$

Then, the monomer concentration in the core region $[M]_c$ could be calculated from eq. (1) as

$$[M]_c = \frac{r^3[M]_p - (r^3 - r_c^3)[M]_s}{r_c^3} \quad (20)$$

where r_c is the radius of core. It would decrease with increasing reaction time due to the fact that more and more monomer diffused outward to the shell region.

The volume of the core (V) in our polymer particle could be described as

$$V = V_{st} + V_{cd} \quad (21)$$

where V_{st} is the volume of the monomer in the core region, and V_{cd} is the volume of the dry polymer in the core region. Equation (21) could be rewritten as

$$V = \frac{[M]_c \cdot V \cdot 104}{905} + \frac{4}{3}\pi \cdot r_{cd}^3 \quad (22)$$

or

$$\frac{4}{3}\pi \cdot r_c^3 = \frac{[M]_c \cdot \frac{4}{3}\pi \cdot r_c^3 \cdot 104}{905} + \frac{4}{3}\pi \cdot r_{cd}^3 \quad (23)$$

or

$$r_c^3 = \frac{r_{cd}^3}{\left(1 - \frac{[M]_c \cdot 104}{905}\right)} \quad (24)$$

where r_{cd} is the radius of the dry PMMA seed. Equation (24) showed that r_c decreased with decreasing $[M]_c$. Substituting eq. (24) into eq. (20), we obtained

$$[M]_c = \frac{905[r^3([M]_p - [M]_s) + r_{cd}^3[M]_s]}{905 \cdot r_{cd}^3 + 104 \cdot r^3([M]_p - [M]_s)} \quad (25)$$

Average Molecular Weight of Polymers

The core–shell polymer composite particles in this work contained PMMA chains in core and PS chains in the shell. The average molecular weight of PS chains was calculated by the equation, as follows:

$$\overline{Mn}_{(ps)} = \frac{x}{\int \frac{x}{\overline{Mn}_i}dx} = \frac{Mx}{\frac{1}{M}\int \frac{Mx}{\overline{Mn}_i}d(Mx)} = \frac{W_{(ps)}}{\frac{1}{M}\int \frac{W_{(ps)}}{\overline{Mn}_i}dW_{(ps)}} = \frac{MW_{(ps)}}{\int \frac{W_{(ps)}}{\overline{Mn}_i}dW_{(ps)}} \quad (26)$$

where $\overline{Mn}_{(ps)}$ is the number-average molecular

weight of PS, x is the conversion, M is the weight of styrene monomer fed into the system, $\overline{Mn}_i$ is the instantaneous number-average molecular weight of PS, and W_{ps} is the weight of PS. $\overline{Mn}_i$ was calculated from instantaneous kinetic chain length $\overline{Xn}_i$ as

$$\frac{\overline{Mn}_i}{104} = 2\overline{Xn}_i = 2\frac{R_p}{R_t} = 2\frac{k_p[M]_s[R\bullet]V_rN}{k_t[R\bullet]^2V_rN} = 2\frac{k_p[M]_s}{k_t[R\bullet]} \quad (27)$$

Factor 2 in the eq. (27) accounted for recombination termination. Assuming steady state for $(R\bullet)$ [i.e., substituting eq. (4) into eq. (27)], then

$$\frac{\overline{Mn}_i}{104} = 2\overline{Xn}_i = 2\frac{k_p[M]_p}{(k_t\rho_i)^{1/2}}V_r^{1/2}N^{1/2} \quad (28)$$

Introducing V_r of eq. (6) into eq. (28), we obtained

$$\overline{Mn}_i = 2 \times 104 \times \frac{k_p[M]_p}{(k_t\rho_i)^{1/2}} \frac{W_p^{1/2}}{\left(\rho_p\left(1 - \frac{[M]_p \cdot 104}{\rho_M}\right)\right)^{1/2}} \quad (29)$$

Substituting eq. (29) into eq. (28), we obtained

$$\overline{Mn}_{(ps)} = \frac{W_{ps}}{\int \frac{(k_t\rho_i\rho_p)^{1/2}\left(1 - \frac{[M]_s \cdot 104}{\rho_M}\right)^{1/2}(0.7608)^{1/2}}{2 \times 104 \times k_p[M]_s \times W_{ps}^{1/2}} dW_{ps}} \quad (30)$$

where $W_{ps} = M \cdot x$.

Equation (30) was available for three regions of polymerization. The important features for three regions were summarized as follows.

1) Region I. $[M]_s = [M]_s^o$ = constant. $k_t = k_{to}$ = constant. $k_p = k_{po}$ = constant.
2) Region II. $[M]_s$ decreased with increasing the conversion as eqs. (11) and (12). k_t decreased with increasing the conversion as eqs. (13) and (14). $k_p = k_{po}$ = constant.
3) Region III. $[M]_s$ decreased with increasing the conversion as eqs. (11) and (12). K_t decreased with increasing the conversion as eqs. (13) and (14). k_p decreased with increasing the conversion as eqs. (16) and (17).

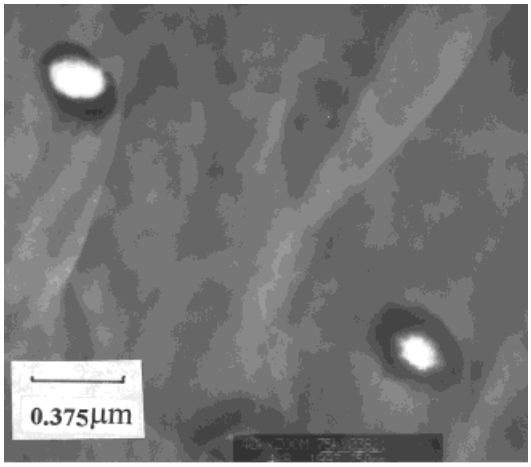

a

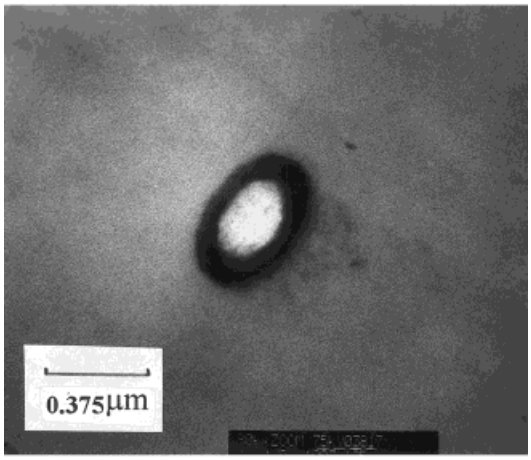

b

Figure 2 TEM photographs of sectioned latex particles at the end of seeded polymerization: (a) seed latex = 49.18 g, EGDMA : MMA = 1 : 85 (mole ratio), $K_2S_2O_8$ = 0.855 g, T = 70°C, ST = 73.77 g (magnification = 75 K); (b) seed latex = 49.18 g, EGDMA : MMA = 1 : 50 (mole ratio), $K_2S_2O_8$ = 0.855 g, T = 70°C, ST = 73.77 g (magnification = 80 K).

RESULTS AND DISCUSSION

Morphology

With lightly crosslinking PMMA latex particle as seeds and $K_2S_2O_8$ as initiator, styrene was poly-

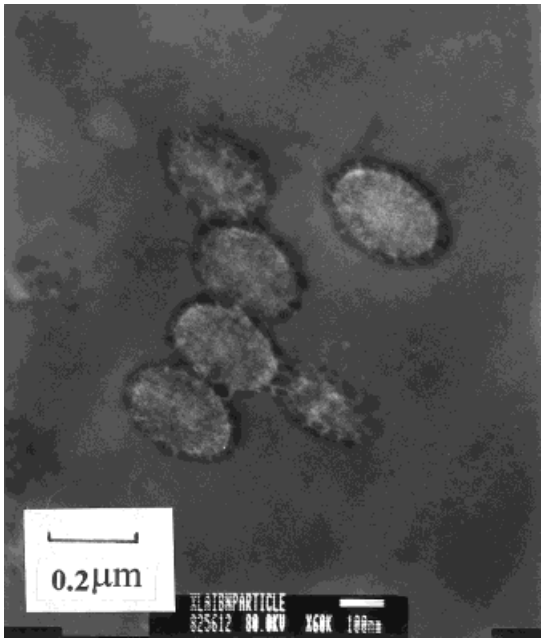

Figure 3 TEM photographs (magnification = 75 K) of sectioned latex particles at the end of seeded polymerization. Seed latex = 49.18 g, EGDMA : MMA = 1 : 50 (mole ratio), AIBN = 0.5 g, T = 70°C, ST = 24.59 g, MMA : ST = 1 : 0.5 (weight ratio).

merized by the method of seeded soapless emulsion polymerization, which formed the PMMA (XL)–PS composite latex. The morphology of the PMMA (XL)–PS composite latex was with the core–shell structure, as seen in Figure 2.

In order to examine the concentration profile of styrene in the crosslinking PMMA seed latex particle during the seeded polymerization, the water-soluble initiator ($K_2S_2O_8$) was replaced by an oil-soluble initiator (AIBN) during the seeded polymerization. In the first stage, we obtained the crosslinking PMMA seed latex as before, then the seed latex was swollen with the mixing solution of styrene and AIBN for 24 hours at room temperature, and then the polymerization of styrene proceeded at 70°C. After the reaction was complete, the composite latex particle was sectioned, stained, and observed under TEM. The morphology of the composite latex particle with AIBN as an initiator showed that PS distributed uniformly in the composite particle, as in Figure 3, from which it indicated that the PMMA seed latex particles were rather uniformly swollen with styrene during the seeded polymerization.

Figure 4 (a)–(c) showed the morphologies of the composite latex particles with different degrees of crosslinking PMMA seeds, as follows: EGDMA : MMA = 1 : 85, EGDMA : MMA = 1 : 30, and EGDMA : MMA = 1 : 5 in mole ratio, respectively.

Figure 4(a) indicated that in the synthesis of the composite latex with lightly crosslinking PMMA seeds, the styrene monomer in the core region of the polymer particle could diffuse outward to the shell region very easily so styrene did not stay in the core region of the composite particle at the end of polymerization.

When the composite latex was synthesized with higher crosslinking PMMA seeds, as seen in Figure 4(b), part of the styrene monomer would trap in the core region on the composite particle because the diffusion of the styrene monomer from core to shell in the latter period of polymerization was hindered by the crosslinking structure of the PMMA seeds.

In Figure 4(c), the composite latex was synthesized in the presence of very high crosslinking PMMA seeds, and no styrene was found in the core region of composite particle. This was because the high degree of crosslinking structure of the core hindered the styrene monomer from diffusing into the PMMA core during the swelling process before the start of the second stage of polymerization, so the styrene monomer could just be polymerized on the shell region of the particle.

Size of Polymer Particles

Figure 5 showed the plot of the average diameter of polymer particles versus conversion with a different degree of crosslinking PMMA seeds over the second stage of polymerization. An increase of conversion (or reaction time) would increase the size of polymer particles, as expected. However, the influence of crosslinking in PMMA seeds on the size of composite polymer particles was insignificant. Figure 6 showed the SEM photograph of PMMA (XL)–PS composite polymer particles with lightly crosslinking PMMA seeds (EGDMA : MMA = 1 : 85) at the end of the second stage of reaction. It indicated that the size distribution of polymer particles was very uniform.

Concentration Distribution of Monomer in Polymer Particle, Core Region, and Shell Region ($[M]_p$, $[M]_c$, and $[M]_s$)

The relation between conversion and concentration of monomer in polymer particles $[M]_p$ was observed from experiments.

The result was shown in Figure 7. In the earlier

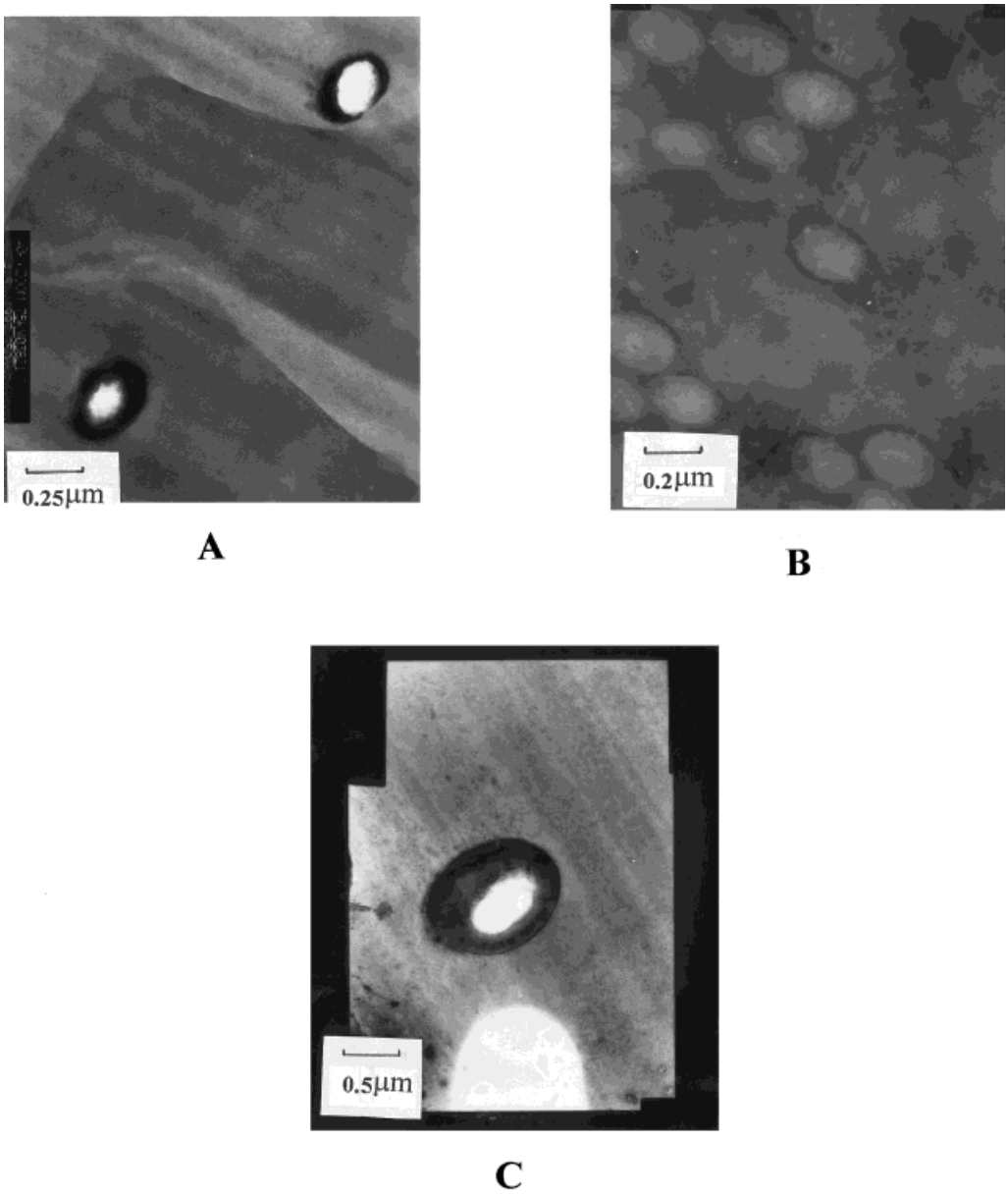

Figure 4 TEM photograph of sectioned latex IPN particles with different degrees of crosslinking PMMA seeds: (a) seed, EGDMA : MMA = 1 : 85 mole ratio; (b) seed, EGDMA : MMA = 1 : 30 mole ratio; (c) seed, EGDMA : MMA = 1 : 5 mole ratio.

period of reaction, monomer droplets still existed in the system, and the concentration of monomer in polymer particles was found to keep at constant value ($[M]_p = [M]_{sa}$). After the monomer droplets disappeared, the concentration of the monomer in polymer particles was unable to retain the saturated concentration; it would decrease linearly with increasing the conversion. The value of $[M]_{sa}$ was about 4.2 mol l^{-1} and about 3.8 mol l^{-1} corresponding to the two reaction systems with different degrees of crosslinking PMMA seeds (EGDMA : MMA = 1 : 85 and EGDMA : MMA = 1 : 50, respectively) at 70°C.

Because the core region was of the crosslinking structure and the shell region was of the linear structure, the monomer concentration in the core region might be different from that in the shell region; that is, $[M]_c \neq [M]_s$. In region I, the monomer concentration in the shell region ($[M]_s = [M]_s^o$) could be obtained from the calculation of the slope of $W_p^{1/2}$ versus t plot [eq. (10)]. The value of $[M]_s^o$ obtained was approximately equal

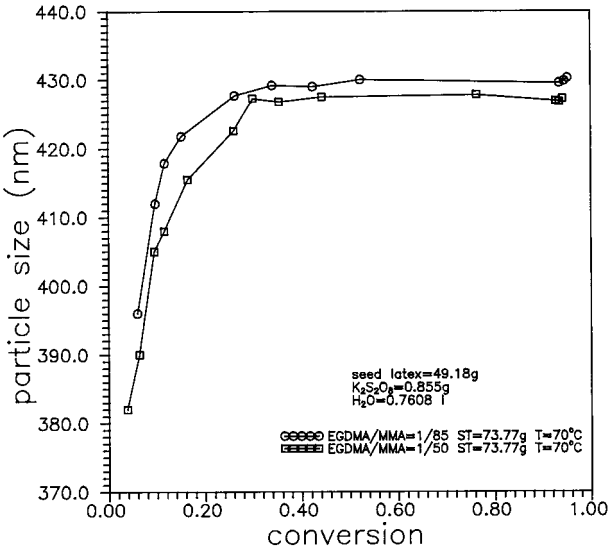

Figure 5 Average diameter of polymer particles versus conversion in the seeded polymerization.

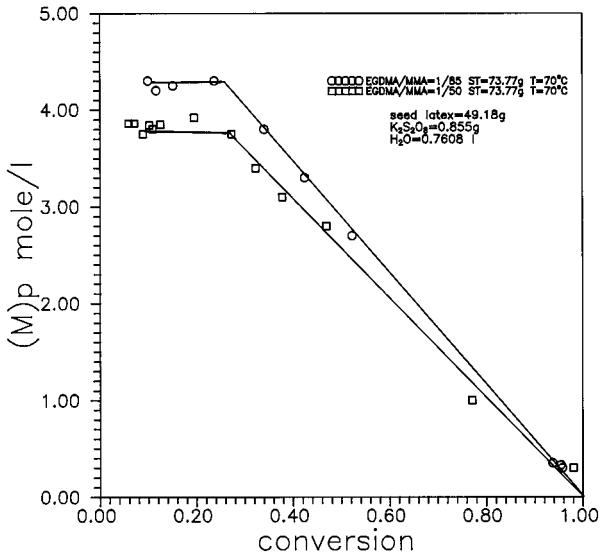

Figure 7 Concentration of the monomer in polymer particles versus conversion in the seeded polymerization.

to $[M]_{sa}$; that is, $[M]_s^o \cong [M]_{sa}$, as shown in Figure 8. Substituting the relation ($[M]_s \cong [M]_p$) into eq. (1), we obtained the result that $[M]_s \cong [M]_p \cong [M]_c \cong [M]_{sa}$ in region I.

But after the monomer droplets disappeared, the monomer inside the polymer particles had to diffuse outward to the surface layer for the reaction of polymerization. Because the core region of the composite polymer particle was of crosslinking structure, which hindered the diffusion of monomer outward to the shell region, the monomer concentration could not distribute in the composite polymer particle uniformly; that is, $[M]_s <\sim [M]_p < [M]_c$. From the calculation of eqs. (11), (12), and (27) for $[M]_s$ and $[M]_c$, the relations between the conversion and the $[M]_s$, $[M]_p$, and $[M]_c$ were shown in Figure 8. It showed that $[M]_s$, $[M]_p$, and $[M]_c$ decreased with increasing the conversion, and $[M]_s < [M]_p < [M]_c$.

Besides, the diameter of the core of the composite polymer particle would decrease with increasing the diffusion of the monomer outward to the shell region. Substituting eq. (25) into eq. (24), we could obtain the relation between the conversion and the diameter of the core, as shown in

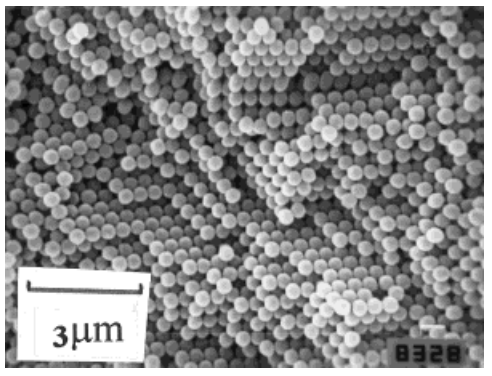

Figure 6 SEM photograph of PMMA–PS latex IPN at the end of seeded polymerization : seed latex = 49.18 g, EGDMA : MMA = 1 : 85 (mole ratio), $K_2S_2O_8$ = 0.855 g, T = 70°C, ST = 73.77 g.

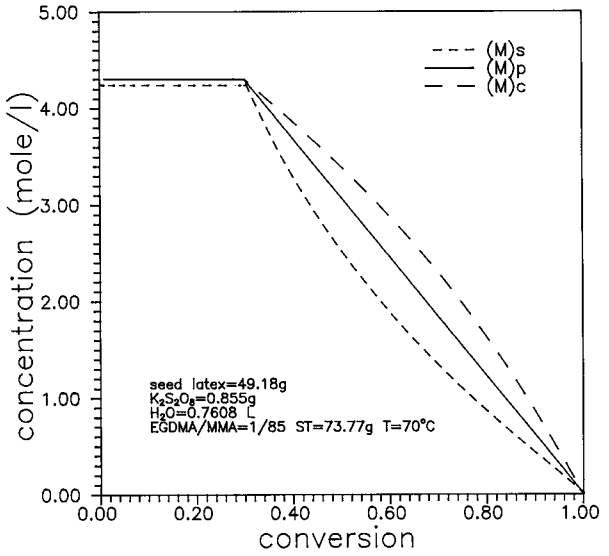

Figure 8 $[M]_p$, $[M]_s$, and $[M]_c$ versus conversion.

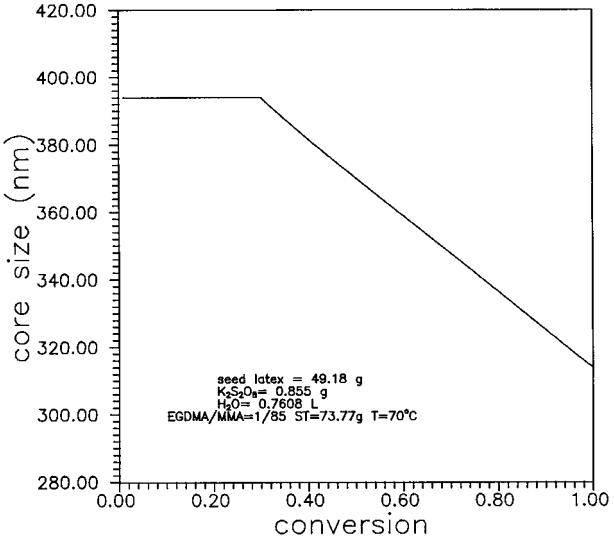

Figure 9 Average diameter of the core region versus conversion in the seeded polymerization.

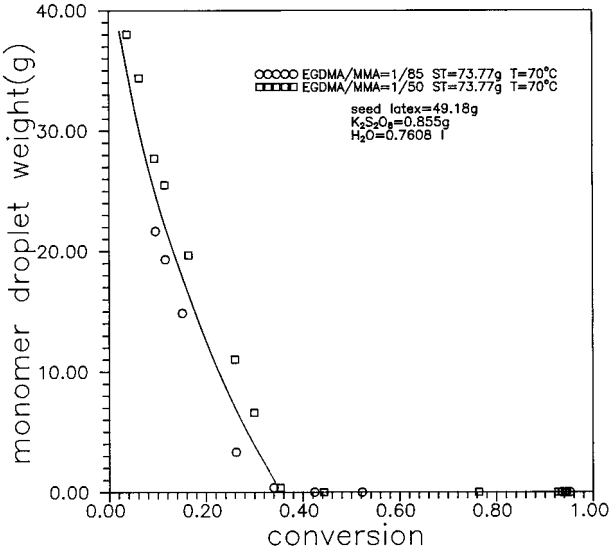

Figure 10 Weight of the monomer droplets in the system versus conversion in the seeded polymerization.

Figure 9. It showed that the diameter of the core remained constant before the monomer droplets disappeared, then decreased linearly with increasing the conversion after monomer droplets disappeared.

Determination of the Onset Conversion (x_c) at Which the Monomer Droplets Disappeared

In order to determine the onset conversion (x_c) at which the monomer droplets disappeared, the mass balance [eq. (31)] was used to calculate the weight of monomer droplets existing in the reaction system. The equation was stated as

$$v_p \cdot [M]_p \cdot N \cdot 0.7608 \cdot 104 + x \cdot M + md = M \quad (31)$$

where the factor 0.7608 is the volume (liter) of water fed into the reaction system, V_p is the average volume of a polymer particle that could be calculated from the diameter of latex particle (the data were shown in Fig. 5), and md is the weight of monomer droplets existing in the reaction system.

Figure 10 showed the plot of conversion versus the weight of monomer droplets over the course of polymerization with different degrees of crosslinking PMMA seeds. It appeared that the monomer droplets disappeared approximately at conversion 0.35. Compared to Figure 7, which showed that the concentration of monomer in polymer particles could not keep at a constant value and began to decrease with increasing the conversion approximately at conversion 0.3. This discrepancy might be due to the fact that when the number of monomer diffusing into the polymer particle was weak, particularly for the crosslinking seeds, the concentration of monomer in polymer particles could not keep at a constant value, although a small amount of monomer droplets still existed in the reaction system. Therefore, we set the onset conversion (x_c) as 0.3 in the calculation of model.

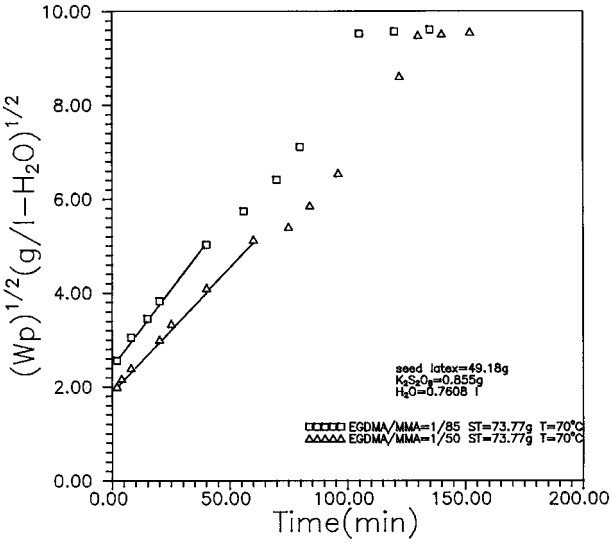

Figure 11 $(W_p)^{1/2}$ versus the reaction time, with different degrees of crosslinking PMMA seeds in the seeded polymerization.

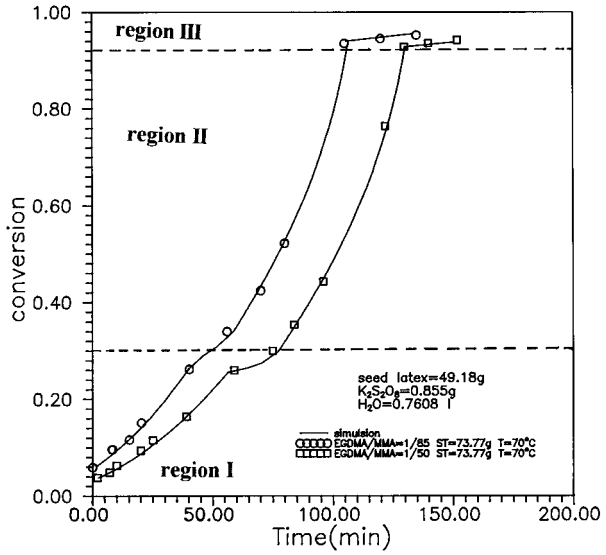

Figure 12 Conversion versus the reaction time, the comparison of core–shell model simulation, and experimental data.

Polymer Yield

Figure 11 showed the experimental data of 0.5 power of the PS yield versus reaction time in the reaction of polymerization with different degrees of crosslinking PMMA seeds. It showed that in the earlier period of reaction (region I), the reaction time was proportional to the 0.5 power of the PS yield. This finding agreed with the relation of polymer yield to reaction time stated in eq. (10).

In region II of the reaction, the effect of crosslinking structure of the core region on the diffusion of monomer was considered; and the empirical eqs. (11) and (12) were used to describe the relation between the monomer concentration in the shell region and the conversion. Besides, the gel effect became important, so the rate constant of termination must be modified by empirical eqs. (13) and (14). Furthermore, when the glassy effect became significant in region III of the reaction, the propagation rate constant (k_p) would also decrease with increasing the conversion, as shown in eqs. (16) and (17).

For the calculation of eqs. (9), (15), and (18) in our core–shell model, together with all the parameters in Table III, the kinetic simulation of conversion by the core–shell model and the experimental data were shown in Figure 12. The results appeared that the conversion prediction by the core–shell kinetic model fitted well with the experimental data. The increases in the degree of crosslinking in PMMA seeds would decrease the rate of polymerization.

Number-Average Molecular Weight of Polymers

Equation (30) was used to calculate the number-average molecular weight of PS polymers in our core–shell model. The parameters were listed in Table III for the calculation. Figure 13 showed the prediction of $\overline{Mn}_{(PS)}$ from eq. (30). It showed that in the latter period of reaction, the glassy effect was significant, and the $\overline{Mn}_{(PS)}$ decreased with increasing the conversion. Besides, with the higher degree of crosslinking in PMMA seeds, a lower number-average molecular weight of PS polymers would be obtained.

CONCLUSION

The morphology of PMMA (XL)–PS composite latex particles synthesized by two-stage soapless emulsion polymerization (i.e., seeded emulsion polymerization) with $K_2S_2O_8$ as the initiator was with the core–shell structure. A modified core–shell model was proposed to predict the conversion over the entire course of polymerization. The model divided the course of polymerization into three regions. Monomer droplets existed in region I, the gel effect was taken into account in region II, and the glassy effect was considered in region III.

The crosslinking structure of the core region

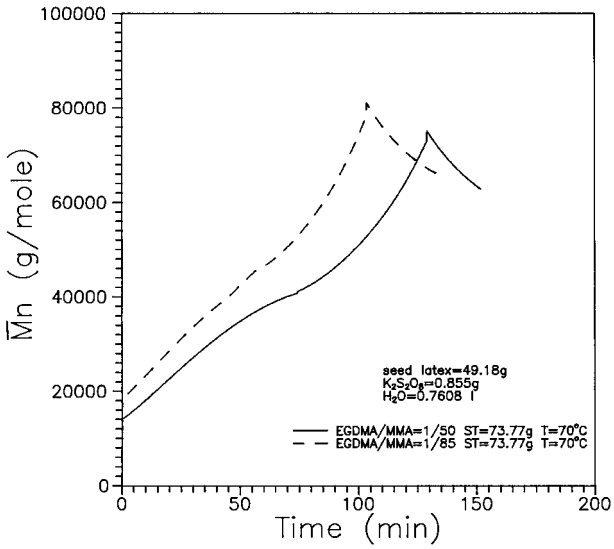

Figure 13 Number-average molecular weight of PS versus the conversion in seeded polymerization.

of the composite polymer particle hindered the diffusion of the monomer, so the monomer concentration in the polymer particle could not distribute uniformly in region II and region III of the reaction. The monomer concentration in the shell region was modified by empirical equations. The prediction on the conversion during the seeded emulsion polymerization on basis of our modified core–shell kinetic model fitted well with the experimental data.

In region I of the reaction, the 0.5 power of the PS yield was proportional to the reaction time. The concentration of monomer in polymer particles was kept constant at 4.2 mol l^{-1} H_2O and 3.8 mol l^{-1} H_2O for two different crosslinking PMMA seeds (EGDMA : MMA = 1 : 50), respectively. After the monomer droplets disappeared, the concentration of monomer in polymer particles would decrease linearly with increasing the conversion.

The size distribution of polymer particles was very uniform. An increase of conversion (or reaction time) would increase the size of polymer particles, as expected. However, the influence of crosslinking of PMMA seeds on the size of composite polymer particles was insignificant.

The number-average molecular weight of PS polymers predicted by the modified core–shell model showed that with higher degree of crosslinking PMMA seeds, the number-average molecular weight of PS polymers formed was lower.

NOMENCLATURE

f	initiator efficiency
$[I]$	initiator concentration (mol L^{-1} H_2O)
k_d	rate constant for initiator decomposition ($L\ min^{-1}$)
k_{po}	propagation rate constant before gel effect took place ($L\ min^{-1}\ mol$)
k_p	propagation rate constant ($1\ min^{-1}\ mol$)
k_{to}	termination rate constant before the gel effect took place ($L\ min^{-1}\ mol$)
k_t	termination rate constant ($L\ min^{-1}\ mol$)
M	weight of the styrene monomer fed into the reaction system (g)
$[M]_o$	initiator monomer concentration (mol L^{-1} H_2O)
$[M]_c$	monomer concentration in core (mol L^{-1})
$[M]_{sa}$	saturated monomer concentration in polymer particle (mol L^{-1})
$[M]_p$	monomer concentration in polymer particle (mol L^{-1})
$[M]_s^o$	monomer concentration in shell (mol L^{-1}) in the reaction of region I
$[M]_c^o$	monomer concentration in core (mol L^{-1}) in the reaction of region I
$[M]_s$	monomer concentration in shell (mol L^{-1})
$\overline{Mn_i}$	instantaneous number-average molecular weight of PS (g mol^{-1})
$\overline{Mn}_{(ps)}$	number-average molecular weight of PS (g mol^{-1})
md	weight of monomer droplets in reaction system (g)
N	particle number per unit volume of water ($L\ L^{-1}$ H_2O)
R_p	rate of polymerization (mol min^{-1} H_2O)
R_t	termination rate of radicals
$[R\cdot]$	concentration of radicals in one polymer particle
r	radius of polymer particle
r_c	radius of core (PMMA + styrene)
r_s	thickness of shell (PS + styrene)
r_{cd}	radius of dry PMMA seed
t	reaction time (min)
V	volume of the core in one polymer particle (L)
V_p	average volume of polymer particles (L)
V_r	volume of reaction zone (L)
V_{st}	volume of the monomer in the core region (L)
V_{cd}	volume of the dry polymer in the core region (L)
W_p	PS yield in seeded polymerization per liter of water (g L^{-1} H_2O)
W_{ps}	weight of PS (g)
x	conversion
x_c	onset conversion at which the monomer droplets disappeared
X_g	onset conversion at which the glassy effect took place
$\overline{Xn_i}$	instantaneous kinetic chain length
ρ_i	generation rate of free radicals (mol min^{-1} H_2O)
ρ_m	density of styrene (st) (g L^{-1})
ρ_p	density of polystyrene (PS) (g L^{-1})

REFERENCES

1. M. S. Silverstein and M. Narkis, *Polym. Eng. Sci.,* **25,** 257 (1985).
2. C. F. Lee and W. Y. Chiu, *J. Appl. Polym. Sci.,* **56,** 1263 (1995).
3. C. F. Lee, W. Y. Chiu, and Y. C. Chern, *J. Appl. Polym. Sci.,* **57,** 591 (1995).

4. C. F. Lee, K. R. Lin, and W. Y. Chiu, *J. Appl. Polym. Sci.,* **51,** 1621 (1994).
5. T. I. Min, A. Klein, M. S. El-Aasser, and J. W. Vanderhoff, *J. Polym. Sci., Polym. Chem. Ed.,* **21,** 2845 (1983).
6. D. I. Lee and T. Ishikawa, *J. Polym. Sci., Polym. Chem. Ed.,* **21,** 147 (1980).
7. R. A. Dickie, M. F. Cheung, and S. Newman, *J. Appl. Sci.,* **17,** 65 (1973).
8. D. J. Hourston, R. Satgurunthan and H. Varma, *J. Appl. Polym. Sci.,* **31,** 1955 (1986).
9. I. Cho and K. W. Lee, *J. Appl. Polym. Sci.,* **30,** 1903 (1985).
10. K. Kato, *Jpn. Plast.,* **2,** 6 (1968).
11. S. L. Rosen, *J. Appl. Polym. Sci.,* **17,** 1805 (1973).
12. U. J. Satbenow and F. Haaf, *Angew. Makromol.,* **29/30,** 1 (1973).
13. P. J. Flory, *Principles of Polymer Chemistry,* Cornell University Press, Ithaca, 1953.
14. H. Tobita and A. E. Hamielec, *Makromol. Chem., Macromol. Symp.,* **35/36,** 193 (1990).
15. D. Zou, V. Derlich, K. Gandhi, M. Park, L. Sun, D. Kriz, Y. D. Lee, G. Kim, J. J. Aklonis, and R. Salovey, *J. Polym. Sci., Polym. Chem.,* **28,** 1909 (1990).
16. D. Zou, S. Ma, R. Guan, M. Park, L. Sun, J. J. Aklonis, and R. Salovey, *J. Polym. Sci., Polym. Chem.,* **30,** 137 (1992).
17. D. Zou, J. J. Aklonis, and R. Salovey, *J. Polym. Sci., Polym. Chem.,* **30,** 2443 (1992).
18. R. H. Shen, M. S. El-Aasster, and J. W. Vanderhoff, **28,** 629 (1990).